

SIGNIFICANCE OF ADC MEASUREMENTS AS RADIOLOGICAL MRI MARKER IN DETECTION OF METASTATIC LYMPH NODE INVOLVEMENT IN PATIENTS WITH PROSTATE CANCER

Yu.O. Mytsyk¹, S.M. Pasichnyk^{1,*}, Yu.S. Kobilnyk¹, O.A. Borzhiievskiy¹, O.E. Lychkovskyy¹, P. Kowal², M. Pietrus², V.M. Matskevych¹, R.I. Dats¹, O.M. Blavatska¹, E.O. Stakhovsky³, A.I. Gozhenko⁴, A.Ts. Borzhiievskiy¹

¹Danylo Halytsky Lviv National Medical University, Lviv 79010, Ukraine

²Department of Urology, Wojewódzki Szpital Specjalistyczny, Wrocław 51-124, Poland

³National Cancer Institute, Kyiv 03022, Ukraine

⁴Ukrainian Research Institute of Transport Medicine of the Ministry of Health of Ukraine, Odesa 65000, Ukraine

Background: In spite of significant advances in diagnosis of prostate cancer (PCa), the detection and differential diagnosis of metastatic lymph node involvement remains an important clinical dilemma in a large number of cases. Contrast-enhanced abdominal computed tomography and magnetic resonance imaging (MRI), in part when using T1-weighted images (T1-WI and T2-WI), allow evaluating indirectly the presence of invasion in regional lymph nodes by assessing their diameter and morphology. Nonetheless, these techniques do not appear to be sufficiently sensitive for direct identification of lymph nodes with metastatic lesions. **Aim:** To study the significance of the apparent diffusion coefficient (ADC) of diffusion-weighted MRI in detection of metastatic lymph node involvement in PCa patients. **Materials and Methods:** The study involved 35 patients with histologically verified PCa. Based on multiparametric prostatic MRI findings and pathomorphological reports, we have performed ADC measurements for pelvic lymph nodes either with ($n = 15$, mean size 1.78 ± 0.59 cm) or without metastases ($n = 20$, mean size: 0.94 ± 0.06 cm) in PCa patients who underwent radical prostatectomy with lymph node dissection. **Results:** No significant differences were observed when comparing mean sizes of N+ and N– pelvic lymph nodes. At the same time, when comparing mean ADC values for N+ and N– pelvic lymph nodes, we observed a statistically significant difference: $0.74 \pm 0.09 \cdot 10^{-3}$ mm²/s in metastatic lymph node vs $1.05 \pm 0.23 \cdot 10^{-3}$ mm²/s in lymph nodes without metastatic involvement ($p < 0.001$). **Conclusion:** The use of ADC for diffusion-weighted MRI may provide valuable information for detection of metastatic lymph node involvement in patients with PCa.

Key Words: prostate cancer, lymph node metastasis, early detection, magnetic resonance imaging, apparent diffusion coefficient.

DOI: 10.32471/exp-oncology.2312-8852.vol-44-no-2.17810

Prostate cancer (PCa) is the second most frequent malignancy in males. On average, approximately 1.1 million PCa cases are diagnosed globally every year, which constitutes 15% of all newly detected cancers [1]. In addition to that, PCa is the second most frequent cause of cancer-related death in males worldwide [2]. The incidence of PCa in European men aged 30–74 years increases by approximately 10–20% every 5 years [3]. In the recent years, the incidence of PCa and the PCa-related mortality in Ukraine has been growing in a steady and catastrophic fashion by +127.4% and +74.3% respectively during the last decade, according to the National Cancer Registry. While the peak of incidence is observed in 65-year-old patients, a substantial fraction of PCa cases has been documented in men of productive age, i.e. 45 to 60 years. 44.7% of all PCa cases detected in Ukraine in 2019 were at the late (IV) stage of the disease, when radical surgical treatment is no longer effective. In the meantime, almost every fifth patient has not survived 1 year after diagnosis [4–7].

Successful PCa treatment largely depends on the accurate diagnosis of the disease. With clinical implementation of a watchful waiting tactics in selected patients with very low and low PCa risk (ISPU 1, GS 6), the precise stratification based on the preoperative assessment is extremely important to avoid excessive treatment [8–13]. However, detection of PCa is still a serious and unresolved clinical problem [14–16].

The detection and differential diagnosis of metastatic lymph node involvement remains a critical clinical issue in many cases, despite significant improvements in the PCa diagnosis. Contrast-enhanced abdominal computed tomography (CT) and magnetic resonance imaging (MRI) using T1-weighted images (T1-WI and T2-WI) allow evaluating indirectly the presence of invasion in regional lymph nodes by assessing their size and morphology. However, these methods do not seem to be sensitive enough to identify directly lymph nodes with metastatic lesions.

Since neither CT nor MRI appear to be sufficiently sensitive for direct identification of positive (i.e. those with metastatic lesions) lymph nodes, a number of approaches to solve this problem have been put forward. The aim of our study was to examine the appropriateness of the apparent diffusion coefficient (ADC) of diffusion-weighted imaging (DWI) MRI in detection of metastatic lymph node involvement in PCa patients.

Submitted: December 06, 2021.

*Correspondence: E-mail: pasichnykdoctua@gmail.com

Abbreviation used: ADC – apparent diffusion coefficient; CI – confidence interval; CT – computed tomography; DWI – diffusion-weighted imaging; mpMRI – multiparametric prostatic MRI; MRI – magnetic resonance imaging; PCa – prostate cancer; PET – positron emission tomography; ROI – region of interest.

MATERIALS AND METHODS

The study involved 35 patients with histologically verified PCa. The mean age was 65.3 ± 6.3 years. The mean PSA level was 11.24 ± 5.35 ng/ml. Based on multiparametric prostatic MRI (mpMRI) findings and pathomorphological reports, we have performed ADC measurements for pelvic lymph nodes both with ($n = 15$, size from 1.53 to 2.85 cm, mean size 1.78 ± 0.59 cm) and without tumor metastases ($n = 20$, size from 0.78 to 1.0 cm, mean size: 0.94 ± 0.06 cm) in patients who underwent radical prostatectomy with lymph node dissection for PCa.

In all cases, pelvic MRI was performed prior to surgical treatment. mpMRI was performed using the Signa DFxt 1.5T scanner (General Electric, USA) and an eight-channel coil in Euroclinic medical centers located in the cities of Lviv, Ivano-Frankivsk and Uzhgorod. Patients abstained from food for 5 h before the test. The night before the test, a small enema (Microlax or similar) was used in all cases. mpMRI was performed using the protocol recommended by the American College of Radiology and PI-RADS clinical guidelines (version 2.1), which included the sequences with the following scan parameters:

Main sequences

1) Axial T2-weighted fast relaxation fast spin echo (FRFSE), repeat time (TR) = 5340 ms, echo time (TE) = 103 ms, flip angle = 90° , field of view (FOV) = 48 cm \times 48 cm, matrix = 200 \times 192;

2) Coronal T2-weighted FRFSE, TR = 5340 ms, TE = 103 ms, flip angle = 90° , FOV = 48 cm \times 48 cm, matrix = 200 \times 192;

3) Sagittal T2-weighted FRFSE, TR = 5340 ms, TE = 103 ms, flip angle = 90° , FOV = 48 cm \times 48 cm, matrix = 200 \times 192;

4) Axial DWI, TR = 6000 ms, TE = 80 ms, FOV = 48 cm \times 48 cm; matrix = 200 \times 192; NEX = 3; bandwidth = 250 kHz; diffusion direction = slice; slice thickness = 3.0 mm; slice gap = 0.3 mm with b-values = 0 and 1000 s/mm²; DWIs were obtained prior to administration of contrast dyes;

5) Axial T1-WI 3D fat-saturated spoiled gradient echo, liver acquisition with volume acquisition (LAVA) with inhibition of fat-derived signal, TR = 4.4 ms, TE = 2.1 ms, flip angle = 15° , FOV = 48 cm \times 48 cm, matrix = 320 \times 192, temporal resolution ≤ 15 s, before and during administration of gadoteric acid at the dose of 0.1 mmol/kg of body weight as bolus injections. In order to reduce the artifacts due to intestinal motility, the patients were given hyoscine butylbromide 20 mg IV immediately before the start of the MRI scan. However, the diagnostic team refrained from administering the drug in patients with a history of glaucoma, acute urinary retention, tachycardia, tachyarrhythmia, heart failure and other manifestations of cardiovascular disease.

Additional sequences

1) Axial T1-weighted Fast spin echo, TR = 640 ms, TE = 7.3 ms, FOV = 48 cm \times 48 cm, matrix = 200 \times 192;

2) Coronal Short-T1 Inversion Recovery with inhibition of fat-derived signal, TR = 4500 ms, TE = 61 ms, FOV = 48 cm \times 48 cm, matrix = 200 \times 192.

The mean duration of an MRI scan was 35 min.

Based on the results of performing DWI sequence, a qualitative data assessment was performed, detecting the areas of diffusion restriction (that is, of limited diffusion), which were represented by foci of hyperintensive MRI signal and were typical for abnormal tumorous lesions, and measuring their sizes. After that, using the maps automatically generated on the workstation based on DWI, we calculated the quantitative parameter, i.e. ADC, which was used as a measure of diffusion of healthy and abnormal tissues.

Statistical analysis was performed using the methods of descriptive statistics (arithmetic mean, standard error of arithmetic mean and confidence intervals). The test for statistical significance of the difference between the means in several groups was performed using a one-way analysis of variance using the ANOVA procedure. The relationships between the parameters were determined using the method for calculation of the Pearson's correlation coefficient. ROC-analysis was used to assess the diagnostic significance of the obtained model and to select the optimal cut-off threshold; the sensitivity and specificity were calculated at a certain threshold value. The critical level (p) for the significance of the null hypothesis was taken as < 0.05 . Microsoft Excel 2016 and IBM SPSS Statistics 22 software packages were used for statistical analysis of the data obtained during the study.

RESULTS

In order to determine ADC, a region of interest (ROI) was established on the ADC map above the required area (prostatic neoplasm, lymph node or normal tissue) with the lowest ADC value identified as the zone with the largest hypo-intensity of MR signal. Taking into consideration that DWIs are morpho-functional images with limited morphological information, in order to improve the accuracy of anatomical comparisons of suspicious areas, we additionally performed mutual overlap of axial T2-WIs and DWIs using RadiAnt DICOM Viewer 2020.2.3 software package, obtaining a color map, where color intensities corresponded to the degrees of diffusion restriction, allowing for accurate spotting of the abnormal lesions detected on DWIs.

To obtain the precise ROI position above the area of the lymph node analyzed on ADC maps, we copied the ROI from the respective slice of axial T1-WIs or T2-WIs, which have served as a precise anatomical landmark. In addition to that, to ensure more precise identification of lymph nodes, we proposed a DWI-based method of pelvic lymph node mapping using a maximum intensity projection algorithm, which facilitated spatial identification of lymph nodes and preoperative preparation (Fig. 1).

No significant differences were observed when comparing mean sizes of N+ and N- pelvic lymph nodes ($p > 0.05$). At the same time, when comparing

mean ADC values for N+ and N- pelvic lymph nodes, we did observe a statistically significant difference: in metastatic lymph node involvement, this value was $0.74 \pm 0.09 \times 10^{-3} \text{ mm}^2/\text{s}$, while in lymph nodes without metastatic involvement this value was $1.05 \pm 0.23 \cdot 10^{-3} \text{ mm}^2/\text{s}$ ($p < 0.001$). Such findings reflect diffusion restriction of hydrogen molecules in N+ lymph nodes due to the increased cellular density in their tissues, which is the case in the development of malignant tumors (Fig. 2). The ROC-analysis using the ADC of DWI MRI for differentiation of N+ and N- pelvic lymph nodes in PCA has shown that in a threshold cut-off value of $0.87 \cdot 10^{-3} \text{ mm}^2/\text{s}$, the sensitivity and specificity were 87% and 75%, respectively, with a high accuracy of the method, area under the curve = 0.933; 95% confidence interval (CI) = 0.852–1.0; $p < 0.001$ (Fig. 3).

DISCUSSION

In spite of the significant advances in PCA diagnosis, detection of metastatic lymph node involvement in most cases remains an important clinical dilemma. Even though contrast-enhanced abdominal CT and MRI allows for indirect evaluation of the lymph nodes with metastatic involvement judging by their size and appearance, the sizes of non-metastatic lymph nodes are highly variable and may overlap with the sizes of nodes with secondary involvement. As a rule, the nodes with the short-axis length of $> 8 \text{ mm}$ in the pelvic area and $> 10 \text{ mm}$ in the extrapelvic area are considered metastatically involved. Reducing these thresholds improves sensitivity, but reduces specificity. Moreover, non-metastatic nodes may become enlarged due to reactive hyperplasia. As a result, the ideal size threshold remains ambiguous [17]. As reported by Zarzour *et al.* [18],

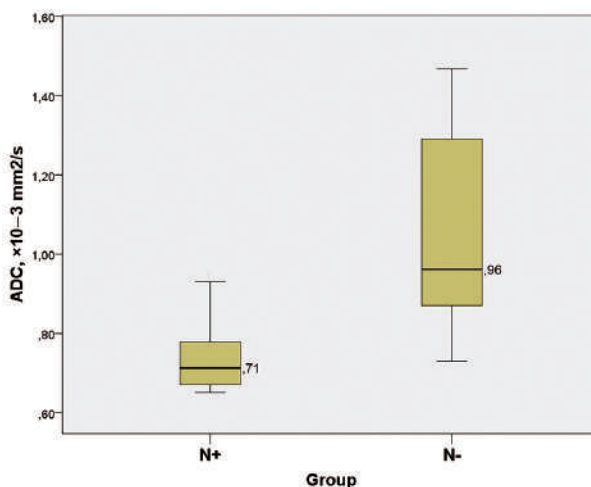


Fig. 2. Box plot and median ADC for N+ and N- pelvic lymph nodes in PCA

CT has demonstrated low sensitivity (42%) and specificity of 82% in detection of metastatic lymph nodes; when MRI was used, these indices were equivalent, with sensitivity of only 39% and specificity of 82%. In a multicenter database, which included 1091 patients, who have had a pelvic lymph node dissection during a radical prostatectomy, the sensitivity and specificity of CT was 8.8 and 98%, respectively [19], which is suboptimal within the context of accurate diagnosis of metastatic lymph node involvement.

Since neither CT nor MRI appear to be sufficiently sensitive for direct identification of the lymph nodes with metastatic lesions, a number of scientists have proposed nomograms that conjoin clinical and biopsy data (for instance, the nomograms developed by Memorial Sloan Kettering Cancer Center, Briganti and

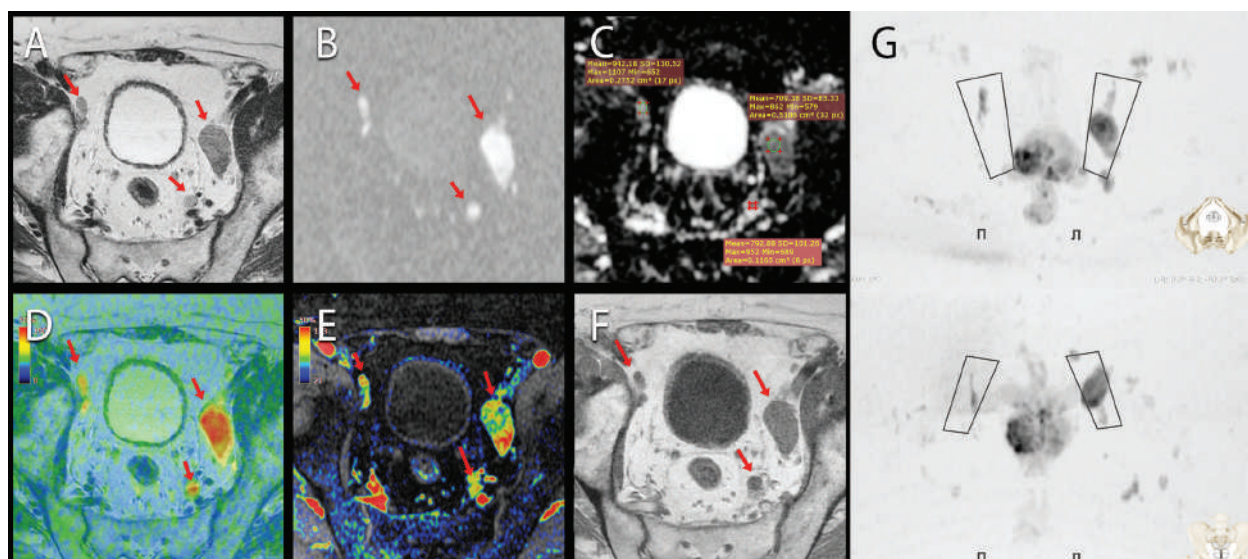


Fig. 1. Prostatic mpMRI of patient S., 65 y.o., with a histologically verified PCA, ISUP 5. Along the left external iliac vessels, there is a group of lymph nodes with diffusion restriction, deposition of contrast dye and sizes $3.7 \times 1.9 \text{ cm}$, $1.4 \times 0.9 \text{ cm}$, that very likely suggests metastatic involvement (see arrows). Along the right external iliac vessels, there is a group of lymph nodes with diffusion restriction; deposition of dye and $2.0 \times 0.6 \text{ cm}$ in the largest dimension, without convincing signs of their secondary involvement (see arrows): A — axial T2-WI; B — axial DWI; C — ADC map, lymph nodes of the left iliac area demonstrate ADC values of $0.71 \cdot 10^{-3} \text{ mm}^2/\text{s}$ and $0.79 \cdot 10^{-3} \text{ mm}^2/\text{s}$, the lymph node of the right iliac area has an ADC value of $0.94 \cdot 10^{-3} \text{ mm}^2/\text{s}$; D — fusion of axial T2-WI and DWI; E — fusion of axial T1-WI LAVA and dynamic contrast enhancement post-processing map using the positive enhancement integral algorithm; F — axial T1-WI; G — DWI-based pelvic lymph node mapping using the MIP algorithm in axial and coronal projections with designations of the right and the left external iliac areas (black trapezoids)

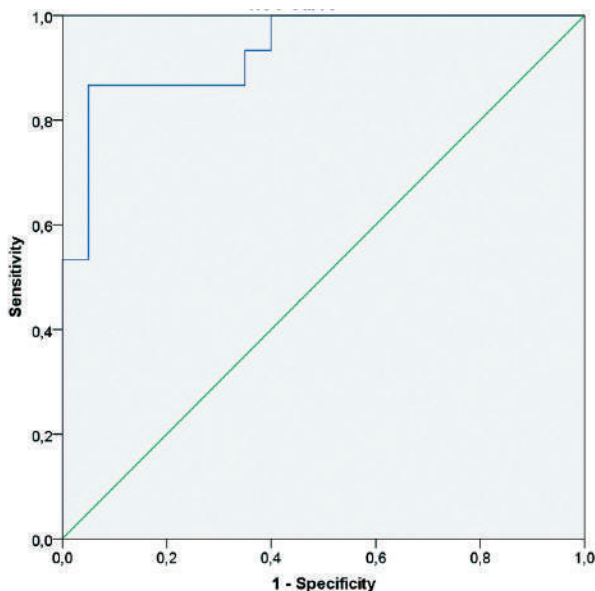


Fig. 3. ROC-curve of ADC in differentiation between N+ and N- pelvic lymph nodes in PCa

Gandaglia), which could be used to identify the patients, who are at higher risk of node invasion and who should be viewed as candidates for lymph node dissection [20–23]. At the same time, the aforementioned instruments are only able to predict the risk of metastatic lymph node invasion in PCa indirectly, showing the accuracies that are far from 100%. Thus, during an external validation of the Briganti nomogram, the area under ROC curves was 79% given the presence of calibration errors [23].

Hybrid modalities, such as positron emission tomography (PET)-CT or PET-MRI may provide valuable information concerning the presence of metastatic involvement of regional lymph nodes and remote metastatic lesions in PCa [24–27]. At the same time, due to limited resolution of PET imaging, this method has low sensitivity in detection of metastatic lymph nodes with the size up to 5 mm [28]. In a study by Wu *et al.* [29], the sensitivity and the specificity of PET-CT with 68 Ga-PSMA in detection of secondary lymph node involvement in PCa were 65% (95% CI: 49–79%) and 94% (95% CI: 88–97%), respectively; while with MRI these parameters were 41% (95% CI: 26–57%) and 92% (95% CI: 86–95%), respectively. However, PET-CT entails exposing the patient to a substantial amount of radiation due to combined effects of X- and γ -rays, which may trigger the development of radiation-induced cancer [30–32]. Thus, Schumann *et al.* [33] observed DNA damage in circulating white blood cells in patients with PCa, who have had a PET-CT assessment with 68 Ga-PSMA. As reported in a large-scale study by Mathews *et al.* [34] (assessing 10.9 million people), performing only one CT test with an average effective radiation dose of 4.5 mSv increased the risk for development of radiation-induced cancer in various organs by 24% compared to the individuals who have never had this test, while the average effective dose when performing PET-CT with 68 Ga-PSMA is 3.54 mSv per patient [35]. Additional limitations for use of PET-CT include the lack of possibility to perform scanning with this

radiopharmaceutical in Ukraine at the time of writing, as well as the low availability of the required equipment in healthcare institutions across the country. A partial solution within the context of balanced diagnostic cost/patient radiation exposure could be provided by hybrid PET-MRI systems [36]; however, such diagnostic systems are currently still unavailable in our country.

Earlier, we have demonstrated a prominent role of MRI and its DWI sequence as a predictive marker of urologic cancers, in particular in renal cell carcinoma [37–39]. There is growing evidence that MRI may play an important role in detection of metastatically involved lymph nodes in patients with PCa. Kiss *et al.* [17] used a multimodal lymph node mapping by means of single-photon emission CT and intraoperative gamma probe following injection of a radioactive isotope (^{99m}Tc nanocolloid) via a flexible cystoscope for detection of metastatic lymph nodes in PCa. They demonstrated that lymphoscintigraphy and the sentinel lymph node concept has limited value for the detection of regional metastases in PCa. In contrast, DWI-MRI allowed for a detection of small lymph node metastases with sensitivity and specificity ranging from 64 to 79% and 79 to 85%, respectively [17]. According to Zarzour *et al.* [18], application of MRI for detection of malignant lymph nodes with short axis diameter of 5–10 mm in patients with PCa demonstrated a sensitivity of 28.5% for MRI alone and 96.4% for MRI plus ferumoxtran-10. In a study by Draulans *et al.* [22], the model based on multiparametric MRI and detailed biopsy information allowed achieving the predictive accuracy for lymph node invasion of 79.7% after five-fold internal cross validation and 72.5% after external validation. In our study, using the ADC of DWI MRI for differentiation of metastatically involved pelvic lymph nodes in PCa has shown the sensitivity and specificity of 87 and 75%, respectively, with a high accuracy, which corresponds to up to date scientific data.

To sum up, the use of ADC for DWI MRI may provide valuable information for detection of metastatic lymph node involvement in PCa patients.

CONFLICTS OF INTEREST

The authors declare no conflicts of interest.

FUNDING

This study was supported by grant of Ministry of Health of Ukraine (registration number O120U101556).

REFERENCES

1. Barsouk A, Padala SA, Vakiti A, *et al.* Epidemiology, staging and management of prostate. *Cancer* 2020; **8**: 28. doi: 10.3390/medsci8030028
2. Pilleron S, Soto-Perez-de-Celis E, Vignat J, *et al.* Estimated global cancer incidence in the oldest adults in 2018 and projections to 2050. *Int J Cancer* 2021; **148**: 601–8. doi: 10.1002/ijc.33232
3. Siegel RL, Miller KD, Jemal A. *Cancer statistics, 2020.* *Cancer J Clin* 2020 **70**: 7–30. doi: 10.3322/caac.21590
4. Fedorenko ZP, Mykhailovych YuI, Hulak LO. *Cancer in Ukraine, 2019–2020.* *Bull Nat Cancer Reg Ukraine* 2019; **22** (in Ukrainian).

5. **Vozianov SO**. Primary overall incidence of and mortality due to the principal genitourinary disease in the context of activity of SI «Institute of Urology of the NAMS of Ukraine». *Urolohiya* 2015; **19**: 15–28 (in Ukrainian).
6. **Vozianov SO, Shamraiev SM, Leonenko AM**. Comparative analysis of the results of retropubic and minimally invasive radical prostatectomy. *Zdorov'e Muzhchiny* 2017; **2**: 29–36 (in Russian).
7. **Chernychenko IO, Lytychenko OM, Tsybaliuk SM, et al**. Investigation of prevalence and incidence of hormone-dependent forms of thyroid cancer, prostate cancer and breast cancer in Ukraine. *Probl Endocr Pathol* 2020; **1**: 72–9 (in Ukrainian).
8. **Hamdy FC, Donovan JL, Lane JA, et al**. 10-Year outcomes after monitoring, surgery, or radiotherapy for localized prostate cancer. *N Engl J Med* 2016; **13**: 1415–24. doi: 10.1056/NEJMoa1606220
9. **Tosoian JJ, Mamawala M, Epstein JI, et al**. Intermediate and longer-term outcomes from a prospective active-surveillance program for favorable-risk prostate cancer. *J Clin Oncol* 2015; **33**: 3379–85. doi: 10.1200/JCO.2015.62.5764
10. **Bruinsma SM, Roobol MJ, Carroll PR, et al**. Expert consensus document: Semantics in active surveillance for men with localized prostate cancer — results of a modified Delphi consensus procedure. *Nat Rev Urol* 2017; **14**: 312–22. doi: 10.1038/nrurol.2017.26
11. **Vozianov SO, Shamraiev SM, Leonenko AM**. Using the National Cancer Institute conditions concept for integral outcome assessment of modified endoscopic radical prostatectomy in patients with localized prostate cancer in a setting of State Institution «Institute of Urology of the NAMS of Ukraine». *Urolohiya* 2020; **24**: 217–21 (in Ukrainian).
12. **Stakhovskiy EO, Vitruk YuV, Voilenko OA, et al**. Finasteride in the prevention of prostate cancer progression. *Zdorov'e Muzhchiny* 2015; **4**: 61–5. (in Russian).
13. **Hryhorenko VM, Vikarchuk MV, Danylets RO, et al**. Prognostic stratification of clinically locally advanced prostate cancer. *Klin Khirurgiya* 2016; **9**: 39–42 (in Ukrainian).
14. **Egevad L, Swanberg D, Delahunt B, et al**. Identification of areas of grading difficulties in prostate cancer and comparison with artificial intelligence assisted grading. *Virchows Arch Int J Pathol* 2020; **477**: 777–86. doi: 10.1007/s00428-020-02858-w
15. **Mishra SC**. A discussion on controversies and ethical dilemmas in prostate cancer screening. *J Med Ethics* 2020; **6**: medethics-2019-105979. doi: 10.1136/medethics-2019-105979
16. **Brönimann S, Prader B, Karakiewicz P, et al**. An overview of current and emerging diagnostic, staging and prognostic markers for prostate cancer. *Expert Rev Mol Diagn* 2020; **20**: 841–50. doi: 10.1080/14737159.2020.1785288
17. **Kiss B, Thoeny HC, Studer UE**. Current status of lymph node imaging in bladder and prostate cancer. *Urology* 2016; **96**: 1–7. doi: 10.1016/j.urology.2016.02.014
18. **Zarzour JG, Galgano S, McConathy J, et al**. Lymph node imaging in initial staging of prostate cancer: An overview and update. *World J Radiol* 2017; **28**: 389–99. doi: 10.4329/wjr.v9.i10.389
19. **Gabriele D, Collura D, Oderda M, et al**. Is there still a role for computed tomography and bone scintigraphy in prostate cancer staging? An analysis from the EUREKA-1 database. *World J Urol* 2016; **34**: 517–23. doi: 10.1007/s00345-015-1669-2
20. **Zelic R, Garmo H, Zugna D, et al**. Predicting prostate cancer death with different pretreatment risk stratification tools: a head-to-head comparison in a nationwide cohort study. *Eur Urol* 2020; **77**: 180–8. doi: 10.1016/j.eururo.2019.09.027
21. **Gandaglia G, Ploussard G, Valerio M, et al**. The key combined value of multiparametric magnetic resonance imaging, and magnetic resonance imaging-targeted and concomitant systematic biopsies for the prediction of adverse pathological features in prostate cancer patients undergoing radical prostatectomy. *Eur Urol* 2020; **77**: 733–41. doi: 10.1016/j.eururo.2019.09.005
22. **Draulans C, Everaerts W, Isebaert S, et al**. Development and external validation of a multiparametric magnetic resonance imaging and international society of urological pathology based add-on prediction tool to identify prostate cancer candidates for pelvic lymph node dissection. *J Urol* 2020; **203**: 713–8. doi: 10.1097/JU.0000000000000652
23. **Gandaglia G, Martini A, Ploussard G, et al**. External validation of the 2019 Briganti nomogram for the identification of prostate cancer patients who should be considered for an extended pelvic lymph node dissection. *Eur Urol* 2020; **78**: 138–42. doi: 10.1016/j.eururo.2020.03.023
24. **Hofman MS, Lawrentschuk N, Francis RJ, et al**. Prostate-specific membrane antigen PET-CT in patients with high-risk prostate cancer before curative-intent surgery or radiotherapy (proPSMA): a prospective, randomised, multicentre study. *Lancet* 2020; **11**: 1208–16. doi: 10.1016/S0140-6736(20)30314-7
25. **Zacho HD, Fonager RF, Nielsen JB, et al**. Observer agreement and accuracy of 18F-sodium fluoride PET/CT in the diagnosis of bone metastases in prostate cancer. *J Nucl Med* 2020; **61**: 344–9. doi: 10.2967/jnumed.119.232686
26. **Werner RA, Derlin T, Lapa C, et al**. 18F-Labeled, PSMA-targeted radiotracers: leveraging the advantages of radiofluorination for prostate cancer molecular imaging. *Theranostics* 2020; **10**: 1–16. doi: 10.7150/thno.37894
27. **Korol PO, Tkachenko MM, Shcherbina OV**. Multimodal imaging of prostate cancer. *Nyrky* 2020; **9**: 68–79 (in Ukrainian).
28. **Mottet N, van den Bergh RCN, Briers E, et al**. EAU-EANM-ESTRO-ESUR-SIOG Guidelines on Prostate Cancer-2020 Update. Part I: screening, diagnosis, and local treatment with curative intent. *Eur Urol* 2021; **79**: 243–62. doi: 10.1016/j.eururo.2021.03.003
29. **Wu H, Xu T, Wang X, et al**. Diagnostic performance of 68Gallium labelled prostate-specific membrane antigen positron emission tomography/computed tomography and magnetic resonance imaging for staging the prostate cancer with intermediate or high risk prior to radical prostatectomy: a systematic review and meta-analysis. *World J Mens Health* 2020; **38**: 208–19 doi: 10.55347
30. **Plouznikoff N, Woff E, Artigas C, et al**. Incidental detection of a radiation-induced soft-tissue sarcoma on 68Ga-PSMA PET/CT in a patient previously treated for prostate cancer. *Clin Nucl Med* 2019; **44**: 501–2. doi: 10.1097/RLU.0000000000002592
31. **Puchalski AL, Magill C**. Imaging gently. *Emerg Med Clin North Am* 2018; **36**: 349–68. doi: 10.1016/j.emc.2017.12.003
32. **Safronova OV, Udatova TV, Kmetiuk YaV, et al**. Evaluation of radiation exposure of pelvic organs when using modern techniques of external beam radiation therapy in radiation treatment of prostate cancer. *Promeneva Diagn Promeneva Terap* 2016; **1**: 65–8 (in Ukrainian).
33. **Schumann S, Scherthan H, Frank T, et al**. DNA damage in blood leukocytes of prostate cancer patients undergoing PET/CT examinations with [68Ga]Ga-PSMA I&T. *Cancers* 2020; **7**: 12.
34. **Mathews JD, Forsythe AV, Brady Z, et al**. Cancer risk in 680,000 people exposed to computed tomography scans in childhood or adolescence: data linkage study of 11 million Australians. *BMJ* 2013; **346**: f2360. doi: 10.1136
35. **Sviriydenka H, Muehlethaler UJ, Nagel HW, et al**. 68Ga-PSMA-11 dose reduction for dedicated pelvic imaging with simultaneous PET/MR using TOF BSREM reconstructions. *Eur Radiol* 2020; **30**: 3188–97. doi: 10.1007/s00330-020-06667-2
36. **Evangelista L, Zattoni F, Cassarino G, et al**. PET/MRI in prostate cancer: a systematic review and meta-analysis. *Eur J Nucl Med Mol Imaging* 2021; **48**: 859–73. doi: 10.1007/s00259-020-05025-0

37. Mytsyk Y, Pasichnyk S, Dutka I, *et al.* Systemic treatment of the metastatic renal cell carcinoma: usefulness of the apparent diffusion coefficient of diffusion-weighted MRI in prediction of early therapeutic response. *Clin Exp Med* 2020; **20**: 277–87. doi: 10.1007/s10238-020-00612-9

38. Mytsyk Y, Borzhiyevskyy A, Dutka I, *et al.* Local recurrence of renal cell carcinoma after partial nephrectomy: applicability of the apparent diffusion coefficient of MRI as an imaging marker — a multicentre study. *Polish J Radiol* 2022; **87**: 325–32. doi: 10.5114/pjr.2022.117593

39. Mytsyk Y, Borzhiyevskyy A, Kobilnyk Y, *et al.* Personalized management of prostate cancer: from molecular and imaging markers to radiogenomics. *Polish J Radiol* 2022; **87**: 58–62. doi: 10.5114/pjr.2022.113204

ЗНАЧЕННЯ РАДІОЛОГІЧНИХ МРТ-МАРКЕРІВ У ВИЯВЛЕННІ МЕТАСТАТИЧНОГО УРАЖЕННЯ ЛІМФОВУЗЛІВ У ХВОРИХ НА РАК ПЕРЕДМІХУРОВОЇ ЗАЛОЗИ

Ю.О. Мицик¹, С.М. Пасічник¹, Ю.С. Кобільник¹,
О.А. Боржівський¹, О.Е. Личковський¹, П. Коваль², М. Г'єструс²,
В.М. Мацкевич¹, Р.І. Дац¹, О.М. Блавацька¹, Е.О. Стаховський³,
А.І. Гоженко⁴, А.Ц. Боржівський¹

¹Львівський національний медичний університет
імені Данила Галицького, Львів 79010, Україна

²Обласна спеціалізована лікарня, відділення урології, Вроцлав,
51-124, Польща

³Національний інститут раку, Київ, 03022, Україна

⁴Український науково-дослідний інститут медицини транспорту
МОЗ України, Одеса 65000, Україна

Стан питання: Рак передміхурової залози (РПЗ) є другим за частотою злоякісним новоутворенням у чоловіків. Незважаючи на значні досягнення в діагностиці РПЗ, виявлення та проведення диференційної діагностики метастатичного ураження лімфатичних вузлів залишається

важливою клінічною дилемою у великій кількості випадків. Комп'ютерна томографія та магнітно-резонансна томографія (МРТ) черевної порожнини з контрастним підсиленням, зокрема з використанням зображень, зважених T1 (T1-WI і T2-WI), дозволяють непрямо оцінити наявність інвазії в регіонарні лімфатичні вузли шляхом оцінки їх діаметру та морфології. **Мета:** Вивчити роль вимірюваного коефіцієнта дифузії дифузно-зваженої МРТ у виявленні метастатичного ураження лімфатичних вузлів у пацієнтів з РПЗ. **Матеріали та методи:** У дослідженні взяли участь 35 пацієнтів з гістологічно верифікованим РПЗ. Середній вік хворих становив $65,3 \pm 6,3$ року. Середній рівень простат-специфічного антигена — $11,24 \pm 5,35$ нг/мл. На основі результатів мультипараметричної МРТ та патоморфологічних досліджень ми визначили вимірюваний коефіцієнт дифузії для тазових лімфатичних вузлів як з ($n = 15$, розмір $1,53\text{--}2,85$ см, середній розмір $1,78 \pm 0,59$ см), так і без метастазів пухлини ($n = 20$, розмір $0,78\text{--}1,0$ см, середній розмір $0,94 \pm 0,06$ см) у пацієнтів, які перенесли радикальну простатектомію з лімфодисекцією з приводу РПЗ. **Результати:** При порівнянні середніх розмірів N+ і N– тазових лімфатичних вузлів достовірних відмінностей не виявлено ($p > 0,05$). Водночас, порівнюючи середні значення вимірюваного коефіцієнта дифузії для N+ і N– тазових лімфатичних вузлів, ми спостерігали статистично значущу різницю: при метастатичному ураженні лімфатичних вузлів це значення становило $0,74 \pm 0,09 \cdot 10^{-3}$ мм²/с, тоді як у лімфатичних вузлах без метастатичного ураження це значення становило $1,05 \pm 0,23 \cdot 10^{-3}$ мм²/с ($p < 0,001$). **Висновок:** Використання вимірюваного коефіцієнта дифузії для дифузно-зваженої МРТ може надати цінну інформацію для виявлення метастатичного ураження лімфатичних вузлів у пацієнтів з РПЗ. Необхідні подальші дослідження з більшою кількістю пацієнтів.

Ключові слова: рак передміхурової залози, метастатичне ураження лімфатичних вузлів, раннє виявлення, магнітно-резонансна томографія, вимірюваний коефіцієнт дифузії.